RESEARCH ARTICLE OPEN ACCESS

Investigations in Effective Viscosity of Fluid in a Porous Medium

W.S. Almalki*, M.H. Hamdan**
*(Department Of Mathematics, Umm Al-Qura University, Saudi Arabia,)
** (Department Of Mathematical Sciences, University Of New Brunswick, Saint John, Canada E2L 4L5)

ABSTRACT
In this work we address the quantification of Brinkman's effective viscosity, which arises due to the presence of the porous medium and its effect on increasing or decreasing the fluid viscosity in relation to the base fluid viscosity. This work is motivated in the main part by the lack of consensus in the available literature on the ranges of effective viscosity. To this end, this work provides a model of quantifying the effective viscosity by incorporating the porous microstructure in the volume-averaged Navier-Stokes equations. Extensive analysis and testing are provided in the current work which considers five different porous microstructures, and the effective viscosity is quantified in each case under Poiseuille flow.
***Keywords* -** Effective Viscosity, Brinkman Equation

I. INTRODUCTION

In spite of the popularity of Darcy's law in the study of groundwater flow, it suffers some limitations that include not accounting for microscopic inertia that arises due to tortuosity of the flow path, [1], [2], [3]. Furthermore, the absence of viscous shear term in Darcy's law limits its ability to account for viscous shear effects that are important when a macroscopic, solid boundary is encountered and on which the no-slip condition is imposed. Darcy's law has been argued to be valid in low permeability, low porosity media where variations at the microscopic, pore-level length scale are negligible at the macroscopic (say, thickness of a porous layer) length scale.

In 1947, Brinkman [4] introduced an extension to Darcy's law by including a viscous term to account for the viscous shear effects that are important in the thin boundary layer near a macroscopic boundary. Accordingly, equations governing the steady flow of a Newtonian fluid through a porous medium composed of a swarm of particles fixed in space are given by the following equation of continuity, and linear momentum equation that is due to Brinkman [4]:

Conservation of Mass:

$$\nabla \bullet \vec{u} = 0. \qquad \ldots(1)$$

Conservation of Momentum (Brinkman's Equation):

$$-\nabla p + \mu^{*}\nabla^{2}\vec{u} - \frac{\mu}{k}\vec{u} = \vec{0} \qquad \ldots(2)$$

where $\vec{u}$ is the ensemble-averaged velocity, μ is the base fluid viscosity, μ^{*} is the viscosity of the fluid saturating the porous medium (i.e. effective viscosity), k is the permeability and p is the pressure. The term $\frac{\mu}{k}\vec{u}$ is the Darcy resistance, and the term $\mu^{*}\nabla^{2}\vec{u}$ is the viscous shear term that facilitates imposition of a no-slip velocity condition on solid boundaries. It is clear that when $\mu^{*} = 0$, Brinkman's equation (2) reduces to Darcy's law.

It has been long realized and documented that there is an increased effective shear viscosity in constricted geometries (such as when a dilute system is present, or as in the pore structure of a porous medium), and close to solid surfaces. Experimental evidence has been summarized and reported in the work of Henniker, (1949), (*cf.* [5] for reference). The literature also reports on experimental and theoretical investigations that provide estimates for $\lambda = \frac{\mu^{*}}{\mu}$ from less than unity to as high as 10, and employ a number of configurations that include flow over spheres, flow in the presence of bounding walls, flow over arrays of circular or elliptic cylinders, and flow through channel-like porous media. Other authors believe that the effective dynamic viscosity arises due to volume averaging and provided detailed theoretical analysis of its quantification. *Alas*; the reported studies provide no definite answer as to what the value of λ should be. However, many agree that the presence of solid walls bounding the porous flow domain, and the geometric configurations of the porous material play an important part in the value of λ, (*cf.* [6], [7], [8], [9], [10], [11], and the references therein).

A number of studies have investigated the validity of Brinkman's equation and a number of excellent and sophisticated analyses have been carried out to quantify the effective viscosity, μ^{*}. Some argue that the viscosity factor, or the ratio, λ, could be greater than unity or less than unity, (*cf.* [1], [12] and the references therein), or could be taken as unity (as favoured by Brinkman [4]). Brinkman initially used Einstein's formula for the viscosity of suspension, [13], [14], to relate fluid viscosity and the effective viscosity, namely

$$\mu^* = [1 + \frac{5}{2}(1 - \varphi)]\mu \qquad \ldots(3)$$

where φ is the effective porosity of the medium (i.e. ratio of volume of interconnected pores to the bulk volume of the medium). **Table 1**, below, is produced using equation (3).

φ	$\lambda = \frac{\mu^*}{\mu} = 1 + \frac{5}{2}(1 - \varphi)$
$\varphi \to 0$	$\lambda \to 3.5$
0.01	3.475
0.5	2.25
0.9	1.25
0.99	1.025
1	1

Table 1. Viscosity Factor λ Based on Einstein's Law for Viscosity of a Suspension

Table 1 illustrates that when $\varphi = 1$, then $\lambda = 1$, or $\mu^* = \mu$. This is the Navier-Stokes flow limit, as this case corresponds to the flow of a Newtonian fluid in free-space, that is, in the absence of the porous matrix. When $\varphi \to 0$, $\mu^* \to \frac{7}{2}\mu$. Clearly, this *should be* the Darcy flow limit. However, Brinkman's equation is supposed to reduce to Darcy's law when porosity is small and $\mu^* = 0$. This could be an indication that equation (3) does not provide a good measure of the effective viscosity in porous media.

Many investigators have attempted to resolve the question of effective viscosity. Some argue that equation (3) is valid for high porosity media (that is, porosity being close to unity). As porosity of the medium decreases, viscosity of the saturating fluid increases. Indeed, the literature includes studies and experiments that report viscosity factors ranging from less than unity to approximately 10, (*cf.* [7], [10], [11] and the references therein). In a recent work, Breugem [12] provided elegant and thorough analysis of the effective viscosity of fluid in a channel-type porous medium and provided the following effective viscosity estimate, referred to here as Breugem's Estimate:

$$\mu^* = \begin{cases} \frac{1}{2}(\varphi - \frac{3}{7})\mu ; \varphi \geq \frac{3}{7} \\ 0 ; \varphi < \frac{3}{7} \end{cases} \qquad \ldots(4)$$

hence, the viscosity factor takes the form:

$$\lambda = \frac{\mu^*}{\mu} = \frac{1}{2}(\varphi - \frac{3}{7}). \qquad \ldots(5)$$

We produce **Table 2** of viscosity factor, below, using equation (5):

φ	$\lambda = \frac{\mu^*}{\mu} = \frac{1}{2}(\varphi - \frac{3}{7})$
0.01	0
0.4	0
0.429	0.0002142857
0.5	0.0357142857
0.95	0.2607142857
0.99	0.2807142857
1	0.2857142857

Table 2. Viscosity Factor Based on Breugem's Estimate

Table 2 shows that the effective viscosity is always less than the base fluid viscosity. When $\varphi \to 1$, Breugem's formula yields an effective viscosity that is less than 30% of the base fluid viscosity. However, one expects that when $\varphi = 1$ the Navier-Stokes flow limit should be reached and $\mu^* = \mu$.

Liu *et al.* [10] studied theoretically and numerically the effects of bounding solid walls on slow flow over regular, square arrays of circular cylinders between two parallel plates. Their results indicate that, between the two limits of the Darcian porous medium and the viscous flow, the magnitude of the viscosity factor λ needs to be close to unity in order to satisfy the non-slip boundary conditions at the bounding walls.

In summary, there seems to be no consensus as to what the viscosity factor should be, nor as to how the effective viscosity could be computed, and how it depends on the porosity of the medium. However, it is agreed upon that the effective viscosity depends on factors that include the type of fluid, the speed of the flow, porosity and permeability of the medium, and the presence of bounding solid walls to the medium.

The above lack of consensus motivates the current work in which we provide analysis of the effective viscosity in flow through porous media. This will be accomplished by analyzing a general model of flow through isotropic porous media that was developed by Du Plessis and coworkers, [1], [2], [15], [16], based on intrinsic volume averaging. We devise a method for evaluating the effective viscosity under Poiseuille flow based on analyzing the geometric factors (porosity functions) of five different types of porous media. Expressions for the effective viscosity, mean velocity, and maximum velocity will be obtained. We also evaluate the viscous flow limit and the Darcy limit, and derive a threshold for the transition from Darcy's to Brinkman's flow regimes. Our goal is to analyze the effect of porosity function on the effective viscosity, with the following objectives:

1) Study the viscosity factor under Poiseuille flow.
2) Analyze the effect of the porous microstructure on the viscosity ratio by considering different types of porous media.
3) Quantify the effects of porosity function on the viscosity ratio.
4) Derive expressions for the velocity distributions, the mean and maximum velocities attained, flow rates, and the necessary driving pressure gradients for the cases of flow through porous media and through free-space.
5) Derive expressions for the viscous flow limit and the Darcy flow limit.

II. MODEL EQUATIONS

A number of authors have derived equations of flow through porous media by averaging the Navier-Stokes equations over a representative elementary volume, REV, and quantifying the frictional forces exerted by the porous medium on the traversing fluid through an idealized description of the porous microstructure, [1], [2], [15], [16]. Letting *V* be the bulk volume of an REV (that is, the combined volume of the solid and pore space), and V_φ the volume of pore space, then porosity of the medium is defined by

$$\varphi = \frac{V_\varphi}{V} . \qquad \ldots(6)$$

Now, for a fluid quantity of interest, *G*, the volume average of *G*, that is the average of *G* over the bulk volume, *V*, is defined by:

$$< G >= \frac{1}{V} \int_{V\varphi} GdV \qquad \ldots(7)$$

and the intrinsic volume average of G, that is the average of *G* over the pore space, V_φ , is defined by

$$G_\varphi =< G >_\varphi = \frac{1}{V_\varphi} \int_{V\varphi} GdV \quad . \qquad \ldots(8)$$

Deviation of the average of *G* from the true quantity *G* is defined by:

$$G^\circ = G - < G > \qquad \ldots(9)$$

and the relationship between the volume average and the intrinsic volume average of *G* is given by:

$$< G >= \varphi < G >_\varphi \equiv \varphi G_\varphi \qquad \ldots (10)$$

The Darcy resistance term can be argued to be dependent on porosity function in order to account for different types of porous structures. What gives rise to the Darcy resistance term in the process of intrinsic volume averaging is a surface integral of the form, [1], [2]:

$$-\frac{1}{V} \int_S [-p^\circ \vec{n} + \mu \nabla \vec{u} \bullet \vec{n}] dS \qquad \ldots(11)$$

where p° is the pressure deviation, $\vec{n}$ is a unit normal pointing into the solid, and S is the surface of the solid within the REV that is in contact with the fluid.

Through their concept of representative unit cell, RUC, Du Plessis and Masliyah, [1], [2], quantified the integral in (11) with the help of a geometric porosity function. In the absence of inertial and gravitational effects, Du Plessis and Masliyah's averaged equations take the following form for constant porosity media, written in terms of the specific discharge, $\vec{q}$:

$$-\nabla p_\varphi + \frac{\mu}{\varphi} \nabla^2 \vec{q} - \frac{\mu}{\varphi} F \vec{q} = 0 \qquad \ldots(12)$$

where $\vec{q} = \varphi \vec{u}_\varphi$ and $\vec{u}_\varphi$ is the intrinsic averaged velocity, p_φ is the intrinsic averaged pressure, F is a porosity function that depends on the porous microstructure and tortuosity of the medium. Du Plessis and Masliyah, [1], [2], argue that hydrodynamic permeability inclusive of nonlinear microscopic inertial effects is given by $k = \frac{\varphi}{F}$. Hydrodynamic permeability is the same as the velocity-independent Darcy permeability for low Reynolds number. Upon using $k = \frac{\varphi}{F}$ in (12), we obtain

$$-\nabla p_\varphi + \frac{\mu}{\varphi} \nabla^2 \vec{q} - \frac{\mu}{k} \vec{q} = 0 \; . \qquad \ldots(13)$$

Now, comparing (13) with (2), we see that if we can identify the Brinkman ensemble averaged velocity, $\vec{u}$, with the specific discharge, $\vec{q}$ and the Brinkman pressure, p , with the intrinsic averaged pressure, p_φ , then $\mu^* = \frac{\mu}{\varphi}$. However, this may not be the case since Brinkman's velocity is an intrinsic velocity. We therefore write (13) in terms of the intrinsic averaged velocity, $\vec{u}_\varphi$, as:

$$-\varphi \nabla p_\varphi + \mu \nabla^2 \varphi \vec{u}_\varphi - \frac{\mu \varphi^2}{k} \vec{u}_\varphi = \vec{0} \qquad \ldots(14)$$

Removing the subscript φ , and dividing equation (14) by the constant porosity φ , we obtain:

$$-\nabla p + \mu \nabla^2 \vec{u} - \frac{\mu \varphi}{k} \vec{u} = \vec{0} \qquad \ldots(15)$$

or in the form

$$-\nabla p + \mu \nabla^2 \vec{u} - \mu F \vec{u} = \vec{0} \qquad \ldots(16)$$

Brinkman's intrinsic velocity and pressure in equation (2) can thus be identified with the intrinsic velocity and pressure of equation (16). We point out that while equation (2) involves the effective viscosity, μ^*, equation (16) does not include μ^* explicitly. However, equation (16) includes a porosity function, *F*. Porosity function (or geometric factor) *F* is dependent on factors such as the porous microstructure, the constituents of the porous matrix (diameter of solid particles), the pore diameter, the porosity of the medium (defined in equation (6)), and tortuosity, *T*, of the medium (defined as the ratio of the pore volume to the pore area). A number of expressions for *F* are available in the literature. Some of these porosity functions are listed in **Table 3**, below, which also gives the corresponding expressions for the hydrodynamic permeability, [15], [16].

Description	Geometric Factor F	Hydrodynamic Permeability $k = \frac{\varphi}{F}$
Granular Matter	$\frac{36(1-\varphi)^{2/3}}{d^2[1-(1-\varphi)^{1/3}][1-(1-\varphi)^{2/3}]}$	$\frac{d^2\varphi[1-(1-\varphi)^{1/3}][1-(1-\varphi)^{2/3}]}{36(1-\varphi)^{2/3}}$
Consolidated Matter	$\frac{42.69(1-T)}{\varphi T^2 d^2}$	$\frac{\varphi^2 T^2 d^2}{42.69(1-T)}$
Unidirectional Fibre Bed	$\frac{24\sqrt{1-\varphi}}{d^2(1-\sqrt{1-\varphi})^2}$	$\frac{\varphi d^2(1-\sqrt{1-\varphi})^2}{24\sqrt{1-\varphi}}$
Ergun's Equation	$\frac{150(1-\varphi)^2}{\varphi^2 d_p{}^2}$	$\frac{\varphi^3 d_p{}^2}{150(1-\varphi)^2}$
Kozeny-Carman Relation	$\frac{180(1-\varphi)^2}{\varphi^2 d_m{}^2}$	$\frac{\varphi^3 d_m{}^2}{180(1-\varphi)^2}$

Table 3. Geometric Factors and Hydrodynamic Permeability.

d_p is the average pore diameter in a channel-like porous material.

d is a microscopic characteristic length.

d_m *is a median diameter of spherical particles.*

In the analysis to follow, we will study the viscosity factor under Poiseuille flow then recover the effective viscosity and view it through analysis of different porosity functions.

III. PLANE POISEUILLE FLOW

Consider the flow driven by a constant pressure gradient, between parallel plates located at *y = -h* and *y = h*, as shown in **Figure 1**.

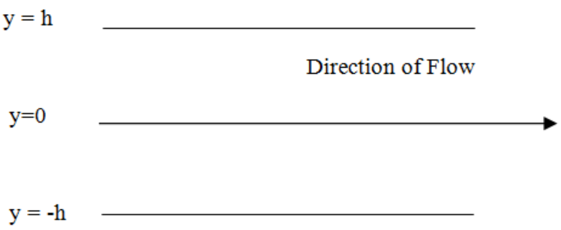

Figure 1. Representative Sketch

When the channel configuration is filled with a fluid-saturated porous material and viscous shear effects are taken into account, the flow is governed by equation (16), which reduces to the following form in which we use $p_x \equiv \frac{dp}{dx}$:

$$u'' - Fu = \frac{1}{\mu} p_x . \qquad \ldots(17)$$

Boundary conditions are no-slip on solid walls, namely

$$u(-h) = u(h) = 0 \qquad \ldots(18)$$

We non-dimensionalize equations (17) and (18) with respect to *h*, and with respect to a characteristic velocity (the mean velocity of the flow, u_m) by defining:

$$u = u_m U\, ;\, y = hY\, ;\, k = h^2 K\, ;\, F = \frac{\varphi}{k} = \frac{\varphi}{h^2 K} = \frac{f}{h^2}\, ;\, f = \frac{\varphi}{K} \qquad \ldots(19)$$

where *k* is the permeability and $K = \frac{k}{h^2}$ is the Darcy number, *Da*, (or dimensionless permeability). In addition, we define:

$$P = \frac{h^2 p_x}{u_m \mu}. \qquad \ldots(20)$$

Equations (17) and (18) are thus expressed in the following dimensionless form, respectively:

$$U'' - fU = P \qquad \ldots(21)$$

$$U(-1)=U(1)=0. \qquad \ldots(22)$$

Factor $f = h^2 F$ that appears in (19) and (21) is critical in the analysis to follow. At the outset, we provide **Tables 4(a)-4(e)** of its values, for a range of porosities, using the expressions for the geometric factor *F* of **Table 3**. These tables provide values for *f* as a function of *h/d*, then specific values are provided when *h/d* takes on the values 10 and 20, for the sake of illustration.

It is clear from **Tables 4(a)-(e)** that *f* increases with increasing *h/d*, and decreases with increasing porosity, until it reaches a value of zero when $\varphi = 1$ (a case that corresponds to flow in free-space, that is in the absence of a porous matrix). In the analysis to follow, the value *f = 0* corresponds to the Navier-Stokes (viscous flow) limit.

Granular Media	$F = \frac{36(1-\varphi)^{2/3}}{d^2[1-(1-\varphi)^{1/3}][1-(1-\varphi)^{2/3}]}$	Values of f for $h/d = 10$	Values of f for $h/d = 20$
φ	$f = Fh^2 = \frac{36(1-\varphi)^{2/3}}{[1-(1-\varphi)^{1/3}][1-(1-\varphi)^{2/3}]}(\frac{h}{d})^2$		
0.1	$14334.95088\,(h/d)^2$	1433495.088	5733980.352
0.5	$297.077457\,(h/d)^2$	29707.7457	118830.9828
0.99	$2.233504\,(h/d)^2$	223.3504	893.401600
0.995	$1.308021611\,(h/d)^2$	130.8021611	523.2086444
0.999	$0.4040404040\,(h/d)^2$	40.40404040	161.6161616
1	0	0	0

Table 4(a). Values of *f* for a range of porosities for granular media.

Consolidated Media		$F=\frac{42.69(1-T)}{\varphi T^2 d^2}$	Values of *f* for *h/d* = 10	Values of *f* for *h/d* = 20
φ	T	$f=Fh^2=\frac{42.69(1-T)}{\varphi T^2}(\frac{h}{d})^2$		
0.1	0.383	$1795.617258\ (h/d)^2$	179561.7258	718246.9032
0.5	0.5	$170.76\ (h/d)^2$	17076	68304.00
0.99	0.993*	$0.306119\ (h/d)^2$	030.6119	122.447600
0.995	0.9966666666	$0.1439733005\ (h/d)^2$	014.39733005	57.58932020
0.999	0.9993333333	$0.02852651259\ (h/d)^2$	002.85265129	11.41060504
1	1	0	0	0

Table 4(b). Values of *f* for a range of porosities for consolidated media.

***Approximated using 3T = 1+2 φ**

Unidirectional Fibre Bed	$F=\frac{24\sqrt{1-\varphi}}{d^2(1-\sqrt{1-\varphi})^2}$	Values of *f* for *h/d* = 10	Values of *f* for *h/d* = 20
φ	$f=Fh^2=\frac{24\sqrt{1-\varphi}}{(1-\sqrt{1-\varphi})^2}(\frac{h}{d})^2$		
0.1	$443.681275\,(h/d)^2$	44368.1275	177472.5100
0.5	$197.824447\,(h/d)^2$	19782.4447	79129.77880
0.99	$2.962963\,(h/d)^2$	296.2963	1185.185200
0.995	$1.965143866\,(h/d)^2$	196.5143866	786.0575464
0.999	$0.8093234225\,(h/d)^2$	080.93234225	323.7293690
1	0	0	0

Table 4(c). Values of *f* for a range of porosities for unidirectional fibre bed.

Ergun's Equation	$F=\frac{150(1-\varphi)^2}{\varphi^2 d_p{}^2}$	Values of *f* for *h/d* = 10	Values of *f* for *h/d* = 20
φ	$f=Fh^2=\frac{150(1-\varphi)^2}{\varphi^2}(\frac{h}{d_p})^2$		
0.1	$12150\,(h/d_p)^2$	1215000	4860000
0.5	$150\,(h/d_p)^2$	15000	60000
0.99	$0.0185185\,(h/d_p)^2$	001.85185	7.4074000
0.995	$0.003787783137\,(h/d_p)^2$	000.3787783137	1.515113255
0.999	$0.0001503004506\,(h/d_p)^2$	000.01503004506	0.06012018024
1	0	0	0

Table 4(d). Values of *f* for a range of porosities using Ergun's equation.

Kozeny-Carman	$F=\frac{180(1-\varphi)^2}{\varphi^2 d_m{}^2}$	Values of *f* for *h/d* = 10	Values of *f* for *h/d* = 20
φ	$f=Fh^2=\frac{180(1-\varphi)^2}{\varphi^2}(\frac{h}{d_m})^2$	$(\frac{h}{d})=10$	$(\frac{h}{d})=20$
0.1	$14580\,(h/d_m)^2$	1458000	5832000
0.5	$180\,(h/d_m)^2$	18000	72000
0.99	$0.0222222\,(h/d_m)^2$	002.22222	8.8888800
0.995	$0.004545339764(h/d_m)^2$	000.4545339764	1.818135906
0.999	$0.0001803605407(h/d_m)^2$	000.01803605407	0.07214421628
1	0	0	0

Table 4(e). Values of *f* for a range of porosities using Kozeny-Carman relation.

Brinkman Velocity Profile

General solution to (21) is given by:

$$U = c_1 \cosh \sqrt{f}\,Y + c_2 \sinh \sqrt{f}\,Y - \frac{P}{f}. \qquad \ldots(23)$$

Using (22) in (23) we obtain $c_1 = \frac{P}{f \cosh \sqrt{f}}; c_2 = 0$ and (23) becomes:

$$U = \frac{P}{f}\left[\frac{\cosh \sqrt{f}\,Y}{\cosh \sqrt{f}} - 1\right]. \qquad \ldots(24)$$

In terms of the dimensional variables, (24) takes the following form in which we leave *f* dimensionless and denote the Brinkman velocity through the porous medium by, u_B :

$$u_B = -\frac{h^2 p_x}{f\mu}\left[1 - \frac{\cosh \sqrt{f}\,y/h}{\cosh \sqrt{f}}\right]. \qquad \ldots(25)$$

The maximum velocity, $u_{\max}$, occurs at $y = 0$ and is given by:

$$(u_B)_{\max} = -\frac{h^2 p_x}{f\mu}\left[1 - \frac{1}{\cosh \sqrt{f}}\right]. \qquad \ldots(26)$$

If the dimensional form of f is used, that is $f = \frac{\varphi h^2}{k}$, equation (25) takes the form:

$$u_B = -\frac{k p_x}{\varphi\mu}\left[1 - \frac{\cosh \sqrt{\frac{\varphi}{k}}\,y}{\cosh \sqrt{\frac{\varphi}{k}}\,h}\right]. \qquad \ldots(27)$$

Darcy Velocity

When the flow is of the seepage type, then it is governed by Darcy's law. In this case, viscous shear effects are ignored and the no-slip on the solid plates is no longer valid. We can obtain the dimensionless Darcy velocity from (21) by setting to zero the viscous shear term, as:

$$U = -\frac{P}{f}. \qquad \ldots(28)$$

Now, from $u_D = u_m U$, where u_D is the dimensional Darcy velocity, and equation (28), we get:

$$u_D = u_m U = -u_m \frac{P}{f} = -\frac{h^2 p_x}{f\mu}. \qquad \ldots(29)$$

Using $f = h^2\varphi / k$ in (29), we obtain:

$$u_D = -\frac{k p_x}{\varphi\mu} \qquad \ldots(30)$$

and upon dividing (30) by u_m, we obtain:

$$u_D / u_m = -\frac{h^2 p_x}{f\mu u_m} = f / f = 1. \quad \ldots(31)$$

Equation (31) provides us with the following observation.

Observation *1:* Darcy velocity u_D is the same as the mean velocity, u_m. This is a constant, uniform velocity across the channel. Furthermore, the maximum Darcy velocity $(u_D)_{\max}$ is also the mean velocity.

Navier-Stokes Velocity

If $f = 0$, that is if $k \to \infty$, equation (21) reduces to the Navier-Stokes flow under Poiseuille conditions. Now, taking $f = 0$ in (21), we obtain the following Navier-Stokes solution satisfying *U(-1)=U(1)=0,* written in terms of the dimensional variables, wherein we denote the Navier-Stokes velocity by u_N:

$$u_N = -\frac{p_x}{2\mu}\left[h^2 - y^2\right] \quad \ldots(32)$$

The maximum velocity, $(u_N)_{\max}$, occurs at $y = 0$ and is given by:

$$(u_N)_{\max} = -\frac{h^2 p_x}{2\mu}. \quad \ldots(33)$$

IV. VOLUMETRIC FLOW RATES AND EFFECTIVE VISCOSITY

The Brinkman volumetric flow rate through the porous medium is denoted here by Q_B, and defined by:

$$Q_B = \int_{-h}^{h} u_B\,dy = \int_{-h}^{h}\left\{-\frac{h^2 p_x}{f\mu}\left[1 - \frac{\cosh\sqrt{f}\,y/h}{\cosh\sqrt{f}}\right]\right\}dy = -\frac{2h^3 p_x}{f\mu}\left\{1 - \frac{\tanh\sqrt{f}}{\sqrt{f}}\right\}. \quad \ldots(34)$$

The Darcian volumetric flow rate through the porous medium is denoted here by Q_D, and defined by:

$$Q_D = \int_{-h}^{h} u_D\,dy = \int_{-h}^{h} -\frac{h^2 p_x}{f\mu}dy = -\frac{2h^3 p_x}{f\mu}. \quad \ldots(35)$$

Upon using (31) in (35), we obtain

$$Q_D = -\frac{2hkp_x}{\varphi\mu} = 2u_D h. \quad \ldots(36)$$

The Navier-Stokes volumetric flow rate is denoted by Q_N, and given by:

$$Q_N = \int_{-h}^{h} u_N\,dy = \int_{-h}^{h} -\frac{p_x}{2\mu}\left[h^2 - y^2\right]dy = -\frac{2h^3 p_x}{3\mu}. \quad \ldots(37)$$

Brinkman's Effective Viscosity in Relation to Base Fluid Viscosity:

In order to find the effective viscosity, μ_B^*, we replace μ by μ_B^* and replace Q_N in (37) by Q_B of (34). This is equivalent to saying: If the Navier-Stokes volumetric flow rate Q_N across the channel is replaced by the Brinkman volumetric flow rate under the same driving pressure gradient and channel depth, what is the corresponding fluid viscosity, μ_B^*?

We thus have:

$$\mu_B^* = -\frac{2h^3 p_x}{3Q_B} = \frac{\mu f}{3 - 3\frac{\tanh\sqrt{f}}{\sqrt{f}}} = \frac{\mu f^{3/2}}{3\sqrt{f} - 3\tanh\sqrt{f}}. \quad \ldots(38)$$

Brinkman's viscosity factor, λ_{BN}, with respect to Navier-Stokes base fluid is defined as:

$$\lambda_{BN} = \frac{\mu_B^*}{\mu} = \frac{f}{3 - 3\frac{\tanh\sqrt{f}}{\sqrt{f}}} = \frac{f^{3/2}}{3\sqrt{f} - 3\tanh\sqrt{f}}. \quad \ldots(39)$$

Darcy's Effective Viscosity in Relation to Base Fluid Viscosity:

In order to find Darcy's effective viscosity, μ_D^*, we replace μ by μ_D^* and replace Q_N in (40) by Q_D of (37).

$$\mu_D^* = -\frac{2h^3 p_x}{3Q_D} = \frac{f\mu}{3}. \quad \ldots(40)$$

Darcy's viscosity factor, λ_{DN}, with respect to Navier-Stokes base fluid, is thus obtained by dividing (40) by μ, namely:

$$\lambda_{DN} = -\frac{2h^3 p_x}{3\mu Q_D} = \frac{\mu_D^*}{\mu} = \frac{f}{3}. \quad \ldots(41)$$

In terms of u_D, μ_D^* takes the form, obtained by substituting (36) in (40): $\mu_D^* = -\frac{h^2 p_x}{u_D}$.

An expression for the Darcy pressure gradient is obtained from (40) or (41) and is of the form:

$$p_x = -\frac{u_D \mu_D^*}{h^2} = -\frac{f\mu u_m}{3h^2}. \qquad \ldots(42)$$

V. FLOW LIMITS AND MEAN VELOCITIES

Viscous Flow Limit

Viscous flow limit corresponds to $\lambda_{BN} = 1$, or $\mu_B^* = \mu$. It is reached when $f \to 0$, or when the permeability approaches infinity, $k \to \infty$. When $f \to 0$, the flow approaches the Navier-Stokes flow and the viscous flow limit is reached. In this case, as $\sqrt{f} \to 0$, $\tanh\sqrt{f} \to \sqrt{f} - \frac{f\sqrt{f}}{3}$ and

$$\frac{f^{3/2}}{3\sqrt{f} - 3\tanh\sqrt{f}} \to \frac{f^{3/2}}{3\sqrt{f} - 3\left(\sqrt{f} - \frac{f\sqrt{f}}{3}\right)} = 1. \qquad \ldots(43)$$

Thus, $\lambda_{BN} = \frac{\mu^*}{\mu} = 1$.

Darcian Flow Limit

The Darcian flow limit corresponds to $\lambda_{BN} = 0$, or $\mu^* = 0$. It is reached when the permeability is small, or $k \to 0$. This corresponds to large values of *f*. The pressure gradient term can be written as:

$$-\frac{h^2 p_x}{\mu u_m} = \frac{f\sqrt{f}}{\sqrt{f} - \tanh\sqrt{f}} = \frac{f}{1 - \frac{\tanh\sqrt{f}}{\sqrt{f}}} \qquad \ldots(44)$$

Now, for large $\sqrt{f}$, $\frac{\tanh\sqrt{f}}{\sqrt{f}} \to 0$ and the pressure gradient takes the form

$$-\frac{h^2 p_x}{\mu u_m} = f. \qquad \ldots(45)$$

This Darcian flow limit depends on Darcy number (*Da*) and the porosity, φ, since $f = h^2\varphi / k = \frac{\varphi}{Da} = \frac{\varphi}{K}$. Equation (45) can thus be written in the form

$$-\frac{p_x}{\mu u_m} = \varphi / k \qquad \ldots(46)$$

and the Darcy permeability may be expressed in the following form:

$$k = -\frac{\varphi\mu u_m}{p_x} \qquad \ldots(47)$$

while the Darcy number can be expressed as:

$$K = Da = -\frac{\varphi\mu u_m}{h^2 p_x} \qquad \ldots(48)$$

It is clear from (47) and (48) that the permeability and Darcy number, respectively, are tied to the medium properties of porosity and channel depth, the driving pressure gradient, and the fluid viscosity. However, the question of how high or low the Darcy number can be chosen in order to make Darcy's law valid, remains to be answered. In what follows we attempt to provide a partial answer in terms of the factor *f*.

Following Bear [4], we express the permeability in the form

$$k = \frac{\varphi h^2}{3} \qquad \ldots(49)$$

From (47) and (49) we have:

$$\frac{k}{\varphi} = \frac{h^2}{3} = -\frac{\mu u_m}{p_x} \qquad \ldots(50)$$

hence we obtain the following expression for the fluid viscosity:

$$\mu = -\frac{h^2 p_x}{3u_m}. \qquad \ldots(51)$$

Now, from (50) and the knowledge that $f = h^2\varphi / k$, we obtain

$$f = h^2\varphi / k = \frac{3}{h^2}h^2 = 3. \qquad \ldots(52)$$

Upon using *f* = 3 in equation (40), namely, $\mu_D^* = -\frac{2h^3 p_x}{3Q_D} = \frac{f\mu}{3}$, we obtain $\mu_D^* = \mu$.

The above analysis furnishes the following observation.

Observation 2: In Darcy's flow, the concept of effective viscosity is irrelevant, or the "effective viscosity" is the same as the base fluid viscosity. Furthermore, the value of $f = 3$ represents the threshold for validity of Darcy's law. With this knowledge, we can determine the value of porosity below which we can assume Darcy's law to be valid.

Mean Velocity

The mean velocity in the channel is the volumetric flow rate per unit depth of the channel. That is,

$$u_m = \frac{Q}{2h}. \qquad \ldots(53)$$

For Navier-Stokes flow, we have

$$u_m = \frac{Q_N}{2h} = \frac{-\frac{2h^3 p_x}{3\mu}}{2h} = -\frac{h^2 p_x}{3\mu} \qquad \ldots(54)$$

and the Navier-Stokes pressure gradient is expressed as:

$$-\frac{h^2 p_x}{u_m} = 3\mu \ . \qquad \ldots(55)$$

For porous medium and the Brinkman flow, we have:

$$u_m = \frac{Q_B}{2h} = -\frac{h^2 p_x}{3f\mu}\left\{3 - 3\frac{\tanh\sqrt{f}}{\sqrt{f}}\right\}. \qquad \ldots(56)$$

The pressure gradient is expressed as:

$$-\frac{h^2 p_x}{\mu u_m} = \frac{3f\sqrt{f}}{\sqrt{f} - \tanh\sqrt{f}} = \frac{3f}{1 - \frac{\tanh\sqrt{f}}{\sqrt{f}}}. \qquad \ldots(57)$$

Now, using equation (43), we see that as $\frac{f^{3/2}}{\sqrt{f} - \tanh\sqrt{f}} \to 1$, $\frac{3f^{3/2}}{\sqrt{f} - \tanh\sqrt{f}} \to 3$.

Hence, $-\frac{h^2 p_x}{\mu u_m} = 3$ when $\sqrt{f} \to 0$; and

$$-\frac{h^2}{u_m} p_x = 3\mu \ . \qquad \ldots(58)$$

This emphasizes the fact that equation (57) reduces to (55) as $\sqrt{f} \to 0$, and the Brinkman flow approaches the Navier-Stokes flow.

The Darcian mean velocity has been obtained from equation (29), and is equal to the Darcy velocity, u_D namely

$$u_m = -\frac{h^2 p_x}{f\mu} = u_D \qquad \ldots(59)$$

and the Darcy pressure gradient is thus expressed as:

$$-\frac{h^2 p_x}{u_m \mu} = f \ . \qquad \ldots(60)$$

Upon using the threshold of validity of Darcy's law, that is f = 3, we obtain transition to Brinkman's flow, and equation (59) yields

$$-\frac{h^2 p_x}{u_m} = 3\mu \ . \qquad \ldots(61)$$

The above analysis furnishes the following observation.

Observation 3*:* Equations (55), (58) and (61) suggest that the Brinkman pressure gradient (with appropriate scaling with respect to the relevant mean velocity and channel depth) approaches the Navier-Stokes pressure gradient when *f = 0*, while the Darcy pressure gradient approaches the Brinkman pressure gradient when *f = 3*.

VI. RESULTS AND DISCUSSION

Tables 6(a) and **6(b)** provide a listing of the values of $-\frac{\mu}{(h^2 p_x)}(u_D)_{\max}$ for *h/d=10* and *h/d=20*, respectively. The **Tables** demonstrate the expected increase inthis quantity with increasing porosity, thus indicating an increase in $(u_D)_{\max}$ with increasing porosity for a given combination of $\frac{\mu}{(h^2 p_x)}$. The maximum Darcy velocity values consistently decrease with increasing *h/d*. These trends persist for all geometric factors considered.

Tables 7(a) and **7(b)** provide a listing of the values of $-\frac{\mu}{(h^2 p_x)}(u_B)_{\max}$ for *h/d=10* and *h/d=20*, respectively. These **Tables** also demonstrate the expected increase in this quantity with increasing porosity, thus indicating an increase in $(u_B)_{\max}$ with increasing porosity for a given combination of $\frac{\mu}{(h^2 p_x)}$. The maximum Brinkman velocity values consistently decrease with increasing *h/d*. These trends persist for all geometric factors considered. Results obtained when using Ergun's equation are close in values to those obtained when using the Kozeny-Carmen relation.

φ	Granular Media	Consolidated Media	Unidirectional Fibre Bed	Ergun's Equation	Kozeny-Carman Relation
0.1	$6.975956935 \times 10^{-7}$	$5.569115554 \times 10^{-6}$	$2.253870191 \times 10^{-5}$	$8.230452675 \times 10^{-7}$	$6.858710562 \times 10^{-7}$
0.5	$3.366125488 \times 10^{-5}$	$5.856172406 \times 10^{-5}$	$5.05498696 \times 10^{-5}$	$6.666666667 \times 10^{-5}$	$5.555555556 \times 10^{-5}$
0.9	$5.420330358 \times 10^{-4}$	$3.878535741 \times 10^{-4}$	$6.160428524 \times 10^{-4}$	$5.40000053 \times 10^{-3}$	$4.50000045 \times 10^{-3}$
0.95	$1.117234799 \times 10^{-3}$	$6.305746742 \times 10^{-3}$	$1.123224337 \times 10^{-3}$	0.024066664	0.020055553
0.99	0.004477269797	0.032667034	$3.374999958 \times 10^{-3}$	0.54000054	0.45000045
0.995	0.007645133625	0.06945732275	0.005088685960	2.640066667	2.200055556
0.999	0.02475000000	0.3505510871	0.01235599974	66.53340000	55.44450001

Table 6(a) Values of *1/f* or $-\frac{\mu}{(h^2 p_x)}(u_D)_{\max}$ **when h/d = 10**

φ	Granular Media	Consolidated Media	Unidirectional Fibre Bed	Ergun's Equation	Kozeny-Carman Relation
0.1	$1.743989234 \times 10^{-7}$	$1.392278888 \times 10^{-6}$	$5.634675477 \times 10^{-6}$	$2.057613169 \times 10^{-7}$	$1.714677641 \times 10^{-7}$
0.5	$8.415313721 \times 10^{-6}$	$1.464043101 \times 10^{-5}$	$1.26374674 \times 10^{-5}$	$1.666666667 \times 10^{-5}$	$1.388888889 \times 10^{-5}$
0.9	$1.35508259 \times 10^{-4}$	$9.696339353 \times 10^{-5}$	$1.540107131 \times 10^{-4}$	$1.350000133 \times 10^{-3}$	$1.125000113 \times 10^{-3}$
0.95	$2.793086998 \times 10^{-4}$	$1.576436686 \times 10^{-3}$	$2.808060842 \times 10^{-4}$	$6.016666165 \times 10^{-3}$	$5.013888471 \times 10^{-3}$
0.99	0.001119317449	0.008166758679	$8.437499895 \times 10^{-4}$	0.135000135	0.11250012
0.995	0.001911283406	0.01736433069	0.001272171490	0.6600166665	0.5500138888
0.999	0.006187500001	0.08763777175	0.003088999936	16.63335000	13.86112500

Table 6(b) Values of *1/f* or $-\frac{\mu}{(h^2 p_x)}(u_D)_{\max}$ **when h/d = 20**

Table 7(a) Values of $\frac{1}{f}\left[1-\frac{1}{\cosh\sqrt{f}}\right]$ **or** $-\frac{\mu}{(h^2 p_x)}(u_B)_{\max}$ **when h/d = 10**

φ	Granular Media	Consolidated Media	Unidirectional Fibre Bed	Ergun's Equation	Kozeny-Carman Relation
0.1	$6.975956923 \times 10^{-7}$	$5.569115554 \times 10^{-6}$	$2.253870191 \times 10^{-5}$	$8.230452675 \times 10^{-7}$	$6.858710562 \times 10^{-7}$
0.5	$3.366125488 \times 10^{-5}$	$5.856172406 \times 10^{-5}$	$5.05498696 \times 10^{-5}$	$6.666666667 \times 10^{-5}$	$5.555555556 \times 10^{-5}$
0.9	$5.420330358 \times 10^{-4}$	$3.878535741 \times 10^{-4}$	$6.160428524 \times 10^{-4}$	0.0053999872	0.0044999974
0.95	$1.117234799 \times 10^{-3}$	0.006305703920	$1.123224337 \times 10^{-3}$	0.0239902854	0.0200211501
0.99	0.004477266900	0.03240864891	0.003374999732	0.2801265977	0.2570934366
0.995	0.007644968641	0.06633376603	0.005088677651	0.4316249033	0.4200852118
0.999	0.02466408936	0.2253243076	0.01235293855	0.4968877718	0.4962698307

Table 7(b) Values of $\frac{1}{f}\left[1-\frac{1}{\cosh\sqrt{f}}\right]$ **or** $-\frac{\mu}{(h^2 p_x)}(u_B)_{\max}$ **when h/d = 20**

φ	Granular Media	Consolidated Media	Unidirectional Fibre Bed	Ergun's Equation	Kozeny-Carman Relation
0.1	$1.743989234 \times 10^{-7}$	$1.392278888\ 10^{-6}$	$5.634675477 \times 10^{-6}$	$2.057613169 \times 10^{-7}$	$1.714677641 \times 10^{-7}$
0.5	$8.415313721 \times 10^{-6}$	$1.464043101 \times 10^{-5}$	$1.26374674 \times 10^{-5}$	$1.666666667 \times 10^{-5}$	$1.388888889 \times 10^{-5}$
0.9	$1.35508259 \times 10^{-4}$	$9.696339353 \times 10^{-5}$	$1.540107131 \times 10^{-4}$	$1.350000133 \times 10^{-3}$	$1.125000113 \times 10^{-3}$
0.95	$2.793086998 \times 10^{-4}$	$1.576436686 \times 10^{-3}$	$2.80806084 \times 10^{-4}$	0.006016635865	0.005013881094
0.99	0.001119317	0.008166503204	$8.4374999\,10^{-4}$	0.1173197961	0.1011172487
0.995	0.001911283	0.01734675428	0.00127217149	0.3048193066	0.2824226878
0.999	0.006187462725	0.08166484371	0.00308899984	0.4877739019	0.4853983784

Tables 8(a) and **8(b)** provide a listing of the values of $-\frac{\mu}{(2h^3 p_x)}Q_B$ for *h/d=10* and *h/d=20*, respectively. These **Tables** demonstrate an increase in this quantity with increasing porosity, thus indicating an increase in the volumetric flow rate Q_B with increasing porosity for a given combination of $\frac{\mu}{(2h^3 p_x)}$. The maximum Brinkman volumetric flow rate values consistently decrease with increasing *h/d*. These trends persist for all geometric factors considered. Results obtained when using Ergun's equation are close in values to those obtained when using the Kozeny-Carmen relation.

The viscosity ratio $\lambda_{BN} = \frac{\mu_B^*}{\mu} = \frac{f}{3 - 3\frac{\tanh\sqrt{f}}{\sqrt{f}}}$ is illustrated in **Tables 9(a)** and **9(b)** for *h/d=10* and *h/d=20*, respectively. Qualitative behavior of the viscosity ratios is illustrated in **Figures 2** and **3**. **Tables 9(a)** and **9(b)** demonstrate an increase in the viscosity ratio with increasing *h/d*, and a decrease with increasing porosity, for all geometric factors considered. When using Ergun's equation and the Kozeny-Carmen relation, the viscosity ratio gets closer and closer to unity as porosity gets closer and closer to unity (the viscous flow limit). When using other geometric factors, the viscosity ratio is still far from unity for the values of *h/d* tested. This points out the need to further decrease the value of *h/d* when these porosity functions are employed. While the case of consolidated media renders moderate results for the viscosity ratio, the value remains close to 2 even when the porosity is close to unity.

In terms of the transition from a Darcy regime to a Brinkman regime, the value of $f = 3$ is reached when the porosity is between 0.98 and 0.985 for the Ergun's equation and the Kozeny-Carmen relation, when *h/d = 10*, and a porosity between 0.991 and 0.992 for *h/d = 20*. For consolidated media, $f = 3$ is reached between the porosity values of 0.998 and 0.999, for *h/d = 10*. It is not reached for *h/d = 20*. For granular media and unidirectional fibres, $f = 3$ cannot be reached for the values *h/d = 10* or *20*. This may be an indication that for these porous structures, transition from Darcy to Brinkman regime occurs at values higher than $f = 3$. Furthermore, these results emphasize the importance of the geometric factors in determining the viscosity ratio and describing the Brinkman flow.

φ	Granular Media	Consolidated Media	Unidirectional Fibre Bed	Ergun's Equation	Kozeny-Carman Relation
0.1	6.9701305 10^{-7}	0.00000555597	0.0000224317	8.222986×10^{-7}	6.85303×10^{-7}
0.5	0.0000334659	0.0000581135767	0.000050190468	0.000066122335	0.0000551414
0.9	0.0005294136	0.0003802151864	0.000600752539	0.005003183133	0.0041981312
0.95	0.0010798911	0.005805015388	0.001085579991	0.02033311723	0.0172153380
0.99	0.0041776690	0.02676297168	0.003178930180	0.1921559994	0.1772746638
0.995	0.0069766702	0.05117053348	0.004725684414	0.2895422254	0.2821444703
0.999	0.0208563206	0.1566939481	0.01098253719	0.3313414418	0.3309459473

Table 8(a) Values of $\frac{1}{f}\left[1-\frac{\tanh\sqrt{f}}{\sqrt{f}}\right]$ **or** $-\frac{\mu}{(2h^3\frac{dp}{dx})}Q_B$ **when h/d = 10**

φ	Granular Media	Consolidated Media	Unidirectional Fibre Bed	Ergun's Equation	Kozeny-Carman Relation
0.1	1.7432609×10^{-7}	0.00000139063	0.0000056213001	2.0566798 10^{-7}	$1.713967615 \times 10^{-7}$
0.5	0.0000083909	0.00001458441	0.0000125925421	0.000016598	0.000013837128
0.9	0.0001339308	0.00009600859	0.0001520994239	0.001300397	0.001087266460
0.95	0.0002746407	0.00151384526	0.0002761005409	0.005549970	0.004658860963
0.99	0.0010818693	0.00742872771	0.0008192412672	0.085825120	0.07496005674
0.995	0.0018277254	0.01507616826	0.001226796297	0.208080090	0.1936379189
0.999	0.0057007871	0.06175409443	0.002917317111	0.325507735	0.3239870180

Table 8(b) Values of $\frac{1}{f}\left[1-\frac{\tanh\sqrt{f}}{\sqrt{f}}\right]$ **when h/d = 20**

φ	Granular Media	Consolidated Media	Unidirectional Fibre Bed	Ergun's Equation	Kozeny-Carman Relation
0.1	4.78231125×10^5	59995.49180	14859.92323	4.05367757×10^5	4.86402826×10^5
0.5	9960.370295	5735.894294	6641.367314	5041.160906	6045.057197
0.9	629.6274019	876.6965266	554.8596330	66.62425190	79.40040824
0.95	308.6730837	57.42161064	307.0555245	16.39361685	19.36257849
0.99	79.78931024	12.45501947	104.8570791	1.734701672	1.880321340
0.995	47.77828414	6.514165686	70.53652005	1.151242562	1.181427844
0.999	15.98236523	2.127289135	30.35121371	1.006011598	1.007213825

Table 9(a) Values of

$$\lambda_{BN} = \frac{\mu_B^*}{\mu} = \frac{f\sqrt{f}}{3\sqrt{f} - 3\tanh\sqrt{f}}$$ **when h/d = 10**

φ	Granular Media	Consolidated Media	Unidirectional Fibre Bed	Ergun's Equation	Kozeny-Carman Relation
0.1	1.91212531×10^6	2.396984663×10^5	59298.26241	1.62073518×10^6	1.944805318×10^6
0.5	39725.56814	22855.45139	26470.69418	20081.98436	24089.77730
0.9	2488.846838	3471.911376	6493.054800	256.3317877	306.5792478
0.95	1213.706779	220.1898310	1207.289679	60.06038053	71.54824666
0.99	308.1086796	44.87085086	406.8805451	3.883866790	4.446812713
0.995	182.3760386	22.10995046	271.7104170	1.601947276	1.721425924
0.999	58.47145752	5.397752753	114.2602332	1.024041205	1.028847808

Table 9(b) Values of

$$\lambda_{BN} = \frac{\mu_B^*}{\mu} = \frac{f\sqrt{f}}{3\sqrt{f} - 3\tanh\sqrt{f}}$$ **when h/d = 20**

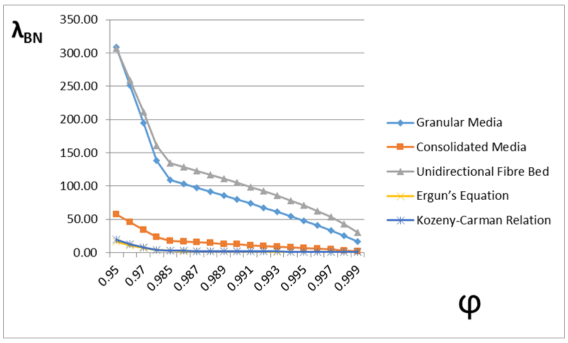

Figure 2 Brinkman Viscosity Ratio, h/d=10

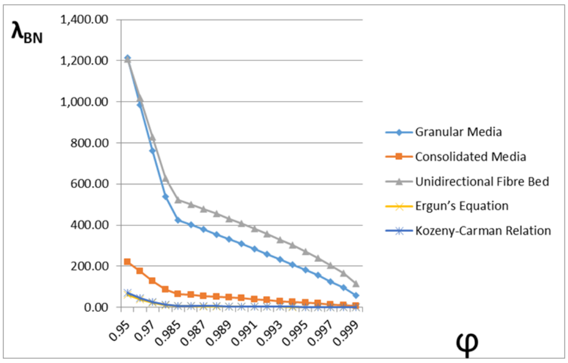

Figure 3 Brinkman Viscosity Ratio, h/d=20

VII. CONCLUSION

In conclusion, we have provided in this work a method of estimating the viscosity factor (hence Brinkman's effective viscosity) based on using different geometric factors (porosity functions) under Poiseuille flow. The most informative results are obtained when using Ergun's equation and the Kozeny-Carmen relation, where results indicate that the viscosity factor approaches unity (or the effective viscosity approaches the base viscosity) as porosity approaches unity (the viscous flow limit). In the analysis we have also determined a threshold value of $f = 3$ to serve as the transition from Darcy to Brinkman flow regime. This value corresponds to value of porosity higher than 98%, thus emphasizing that Brinkman's equation is possibly valid for high values of porosity.

REFERENCES

[1]. J.P.Du Plessis and J.H.Masliyah, Mathematical modeling of flow through consolidated isotropic porous media, Transport in Porous Media, 3 (1988), 145-161.
[2]. J.P.Du Plessis and J.H.Masliyah, Flow through isotropic granular porous media, Transport in Porous Media, 6 (1991), 207-221.
[3]. J.L. Auriault, On the domain of validity of Brinkman's equation, Transport in Porous Media, 79 (2009), 215–223.
[4]. H.C.Brinkman, A Calculation of the viscous force exerted by a flowing fluid on a dense swarm of particles, Applied Scientific Research, A1 (1947), 27-34.
[5]. S.C. Cowin, The theory of polar fluids, Advances in Applied Mechanics, 14 (1974), 279–347.
[6]. J. Francisco, J. Valdes-Parada, Alberto Ochoa-Tapia and Jose Alvarez-Ramirez, On the effective viscosity for the Darcy–Brinkman equation, Physica A, 385 (2007), 69–79.
[7]. R.C. Givler and S.A. Altobelli, A determination of the effective viscosity for the Brinkman-Forchheimer flow model, Journal of Fluid Mechanics, 258 (1994), 355-370.
[8]. J.A.Kolodziej, Influence of the porosity of a porous medium on the effective viscosity in Brinkman's filtration equation, Acta Mechanica, 75 (1988), 241-254.
[9]. J. Koplik, H. Levine and A. Zee, Viscosity renormalization in the Brinkman equation, Physics of Fluids, 26 (1983), 2864-2870.
[10]. H.Liu, P.R.Patil and U. Narusawa, On Darcy-Brinkman equation: viscous flow between two parallel plates packed with regular square arrays of cylinders, Entropy, 9 (2007), 118-131.
[11]. N. Martys, D.P. Bentz and E.J. Garboczi, 1994 Computer simulation study of the effective viscosity in Brinkman's equation, Physics of Fluids, 6(4) (1994), 1434-1439.
[12]. W.-P. Breugem, The effective viscosity of a channel-type porous medium, Physics of Fluids, 19(10) (2007), 103103-1- 103104-8.
[13]. A.Einstein, EineneueBestimmung der Molek¨uldimensionen, Annalen der Physik, 19 (1906), 289-306.
[14]. A.Einstein, 1911 Berichtigungzumeiner Arbeit: "Eineneue Bestimmungder Molek¨uldimensionen.", Annalender Physik, 34 (1911), 591-592.
[15]. J.P.Du Plessis, Analytical quantification of coefficients in the Ergun equation for fluid friction in a packed bed, Transport in Porous Media, 16 (1994), 189-207.
[16]. J.P. Du Plessis and G.P.J.Diedericks, Pore-scale modeling of interstitial phenomena. In "Fluid Transport in Porous Media", J.P.Du Plessis, ed., Computational Mechanics Publications, 1997, 61-104.